CARBON 49 (2011) 3553–3559

available at www.sciencedirect.com

ScienceDirect

journal homepage: www.elsevier.com/locate/carbon

Reinforcing effects of adding alkylated graphene oxide to polypropylene

Young Soo Yun, Yo Han Bae, Do Hyeong Kim, Jae Yun Lee, In-Joo Chin, Hyoung-Joon Jin *

Department of Polymer Science and Engineering, Inha University, Incheon 402-751, South Korea

ARTICLE INFO

Article history:
Received 21 December 2010
Accepted 8 April 2011
Available online 22 April 2011

ABSTRACT

This study examined the reinforcing effects of alkylated graphene oxide (AGO) on a non-polar polypropylene (PP) matrix, and compared these effects with those of one-dimensional carbon nanotubes (CNTs). The surface of graphene oxide was modified with a linear alkyl chain via a bimolecular nucleophilic substitution reaction between the oxygen groups of GO and the reactants to promote the homogeneous dispersion of GO in an organic solvent and increase the interfacial adhesion between the GO and non-polar polymer matrix. The thermal degradation temperatures (TDTs), re-crystallization temperatures and Young's modulus of PP were increased by the incorporation of AGO. In particular, the TDTs were increased by more than 33 °C with the addition of 1 wt% AGO to PP. The addition of only 0.1 wt% AGO increased the Young's modulus of the PP by more than 70%. These reinforcing effects of AGO were different from those of the one-dimensional alkylated CNTs. These superior reinforcing effects were attributed to the two-dimensional structure of AGO as well as the good interfacial adhesion between the AGO and PP matrix.

1. Introduction

Carbon based reinforcing fillers with different shapes, sizes and dimensions have been studied extensively in the field of polymer composites [1–3]. In particular, the mechanical, thermal and electrical properties of carbon nanotube-reinforced polymer composites were enhanced due to the superb physical properties and high aspect ratio of CNTs. In this case, the reinforcing effects are dependent on the morphological characteristics [4–7]. One-dimensional CNTs with a long static bending persistence length (l_P) and high aspect ratio are more beneficial to the percolation of a two-dimensional network. Therefore, the properties of polymer composites reinforced with CNTs with a long l_P and high aspect ratios can be improved greatly at low filler contents.

Graphene, a new class of two-dimensional carbon nanostructure, has attracted considerable attention owing to its unique physical, chemical and mechanical properties [8–10], such as high mechanical strength (>1060 Gpa), high thermal conductivity (~3000 W/m K), high electron mobility (15,000 $cm^2/V\,s$) and high specific surface area (2600 m^2/g) [11–14]. The unique nanostructure and properties have potential applications in polymer composites. Recently, there are several reports related to graphene/polymer composites [15–19]. When incorporated, graphene improved significantly the electrical, thermal and mechanical properties of the host polymers at a small loading. Stankovich et al. reported the lowest electrical percolation threshold of 0.1 vol% for a polystyrene matrix [17]. Veca et al. achieved an up to 30-fold increase in thermal conductivity by incorporating 33 vol% for epoxy [18]. In addition, Rafiee et al. reported the enhancement of Young's modulus and tensile strength by ~31% and ~40%, respectively [19]. Graphene oxide (GO) is easily available through the controlled chemical oxidation of graphite. GO contains graphitic domains and oxidation regions, in which the epoxide and hydroxyl groups are located on the basal

* *Corresponding author:* Fax: +82 32 865 5178.
E-mail address: hjjin@inha.ac.kr (H.-J. Jin).
0008-6223/$ - see front matter
doi:10.1016/j.carbon.2011.04.055

planes, and carbonyl and carboxyl groups are found at the edges [20,21]. The presence of these functional groups makes graphene oxide sheets strongly hydrophilic, which allows GO to readily swell and disperse in water. In addition, the oxygen functionality allows for enhanced interactions with the polar polymer matrices. The ability of GOs to disperse well and interact intimately with polar polymers, such as PMMA, creates a percolated domain of an 'interphase' polymer that affects dramatically the thermal and mechanical properties at loadings as low as 0.05 wt% [22]. However, GOs require surface modification to disperse in non-polar polymers, such as polyethylene, polypropylene (PP) and polystyrene. Fortunately, the surface modification of GO can be induced easily with functional groups, such as epoxide, hydroxyl and carboxyl groups [23,24].

In this study, the reinforcing effects of alkylated graphene oxide (AGO) on the non-polar PP matrix were examined and compared with the reinforcing effects of one-dimensional CNT. The surface of GO was modified using a linear alkyl chain from a simple organic reaction to disperse the GO homogeneously in an organic solvent and increase the interfacial adhesion between GO and the non-polar polymer matrix. Two-dimensional AGO enhanced the thermal properties of PP and had a partial effect on its mechanical properties.

2. Experimental

2.1. Preparation of alkylated graphene oxide

GO was prepared from natural graphite (Sigma–Aldrich) using the Hummers method. Aqueous GO suspensions were frozen in liquid nitrogen and then freeze-dried using a lyophilizer (LP3, Jouan, France) at −50 °C and 0.045 mbar for 72 h. After lyophilization, low density, loosely packed GO powders were obtained. 100 mg of the GO powders were exfoliated under ultrasonication in 180 mL of deionized water containing 72 mg of NaOH. Subsequently, 100 mg of a phase transfer agent, tetra-*n*-octylammonium bromide (TOAB, Fluka), and 5.0 mL of dodecyl iodide (Aldrich, 98%) were added to the black homogeneous sodium salt mixture. After stirring for six hours at 80 °C, a black precipitate was obtained. The precipitate was filtered with excess chloroform, washed several times with a 15% NaCl aqueous solution and dried under vacuum. Fig. 1 shows the alkylation reaction.

2.2. Preparation of polypropylene/alkylated graphene oxide composite

PP was purchased from Sigma–Aldrich; the compound had a number average molecular weight, Mn, of 50,000 and a mass average molecular weight, Mw, of 190,000. Five different types of AGO/PP composites, containing 0.1, 0.3, 0.5, 0.7 and 1.0 wt% AGO were prepared to examine the reinforcing effects according to different filler contents. The nomenclature of these five composites was AGO-01/PP, AGO-03/PP, AGO-05/PP, AGO-07/PP and AGO-10/PP.

The AGO/PP composites were prepared using the follow method. First, PP was added to a 3-neck round flask containing xylene. The flask was placed in an oil bath at 130 °C under a nitrogen atmosphere. AGO was dispersed homogeneously in xylene before being added to the flask. The xylene suspension was ultrasonicated for 30 min at room temperature using an ultrasonic generator (Kodo Technical Research Co., NXCS-600, KOREA) with a frequency and nominal power of 28 kHz and 600 W, respectively. After the PP has been dissolved in xylene at 130 °C, the xylene suspension containing the AGO was dropped into the PP solution. After stirring for 30 min, the mixture was precipitated with excess methanol until a gray AGO/PP composite solid was obtained. The composites were washed several times with methanol, and were dried in a vacuum oven for 72 h at 70 °C.

2.3. Characterization

The morphology of GO was observed by transmission electron microscopy (TEM, CM200, Philips, USA) and atomic force microscopy (AFM, a Digital Instrument Nanoscope IVA). The structure of GO and AGO was examined by Fourier transform infrared spectroscopy (FT-IR, VERTEX 80v, Bruker Optics, Germany). X-ray photoelectron spectroscopy (XPS, PHI 5700 ESCA) was performed using monochromated Al Kα radiation ($h\nu$ = 1486.6 eV). Differential scanning calorimetry (DSC, Perkin-Elmer 7) was carried out in dry nitrogen gas at a flow rate of 10 mL/min. The DSC was calibrated using indium as the standard, and the sample weight was 7.0 ± 0.1 mg. The thermal history of the products was removed by scanning them from 30 to 220 °C at a heating rate of 10 °C/min followed by cooling to 25 °C at a scan rate of 10 °C/min. The quantity of alkyl chains introduced to the AGO and the thermal degradation behavior of the composites was calculated by thermogravimetric analysis (TGA, Q50, TA instruments, UK)

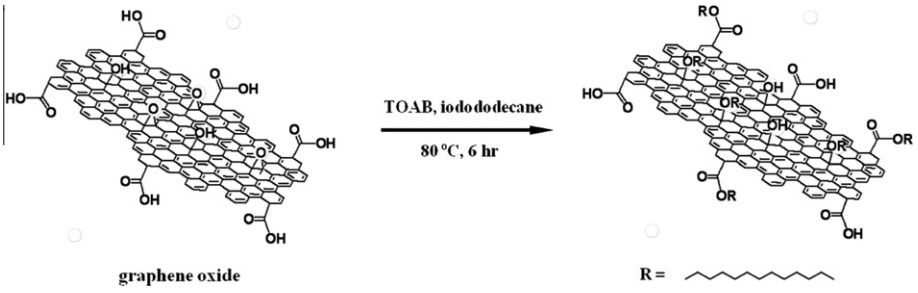

Fig. 1 – Alkylation reaction of graphene oxide using a linear alkyl chain.

at temperatures ranging from 20 to 800 °C at a heating rate of 10 °C/min under a nitrogen atmosphere. The tensile properties were tested using an Instron 4665 ultimate tensile testing machine (UTM) at 20 °C and a humidity of 30%. The dumb-bell specimens were made according to the ASTM D 638 standard for tensile testing. The cross-head speed was set to 50 mm/min for both the dumb-bell samples. The mean value of each product was determined as the average value of five test specimens.

3. Results and discussion

Fig. 2 shows the morphology of the GO. GO exhibited a two-dimensional sheet morphology, which had a thickness and mean lateral size of <2 and 850 nm, respectively. The surface functional groups of the GO were modified to linear alkyl chains to disperse them homogeneously in an organic solvent and increase the interfacial adhesion between GO and the non-polar polymer matrix.

AGO was prepared by a S_N2 reaction between the oxygen groups of GO and the reactants. The existence of alkyl groups incorporated on the surface was confirmed by FT-IR spectroscopy. Fig. 3 presents the FT-IR spectra of GO (a) and AGO (b). Peaks corresponding to the presence of hydroxyl and carboxyl groups were observed at 3455 and 1727 cm^{-1} in the GO, and the peaks at 1110 and 1086 cm^{-1} were assigned to epoxide groups on the surface. These peaks indicate the oxidation of graphite by concentrated acid. The functional groups induced by oxidation allow GO to readily swell and disperse in water. Consequently, GO is exfoliated by ultrasonication in water and the functional groups of GO provide reaction sites for the alkyl groups. In the case of AGO, the bands at 2924 and 2852 cm^{-1} were assigned to the CH_2 stretching vibration and the peak at 1457 cm^{-1} was attributed to the CH_3 degeneration deformation. These peaks suggest the presence of alkyl groups on the GO surface.

Fig. 4 shows the high-resolution C 1s XP spectra of GO (a) and AGO (b). The C 1s XP spectrum of GO (Fig. 3(a)) clearly shows a considerable degree of oxidation with four components corresponding to carbon atoms with different functional groups: non-oxygenated ring C, C in C—O bonds, carbonyl C and carboxylate carbon (O—C=O). Although the C 1s XPS spectrum of AGO (Fig. 3(b)) also showed the same

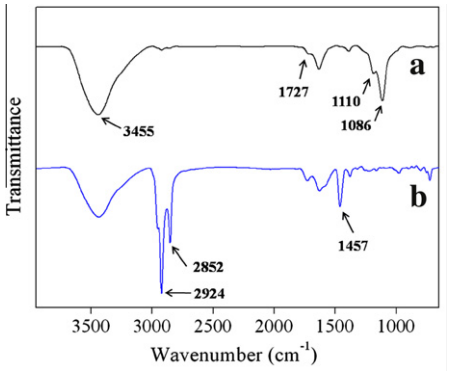

Fig. 3 – IR spectra of graphene oxide (a) and alkylated graphene oxide (b).

oxygen-containing functionalities, the peak intensities of the C—C bonds were much higher than those in GO, confirming the successful incorporation of alkyl groups.

The degree of functionalization of GO and AGO was characterized by TGA (Fig. 5). The TGA curve of GO showed obvious weight loss between 120 and 230 °C, which was attributed to the loss of oxygen functional groups on the GO. In the case of AGO, weight losses of oxygen groups and alkyl chains were observed between 180 and 480 °C. The difference in weight loss between GO and AGO indicates the contents of alkyl groups incorporated on the GO, which comprise approximately 22%. These alkyl groups make AGO hydrophobic, which allows AGO to disperse readily in organic solvents.

Fig. 6 shows an optical image of the AGO dispersions in different solvents, from non-polar solvents, such as toluene to polar solvents, such as water. GO was dispersed in both polar aprotic solvents with a high dipole moment and polar protic solvents [25–27].

In contrast to the case of GO, AGO was dispersed homogeneously in non-polar solvents containing xylene but not in polar solvents, such as methanol and water. The ability of AGOs to disperse well and interact intimately with the hydrophobic polymer matrixes can easily create a percolated domain of AGOs, which affects the thermal and mechanical properties dramatically at low filler loading. AGO/PP composites were prepared using AGO dispersions in xylene.

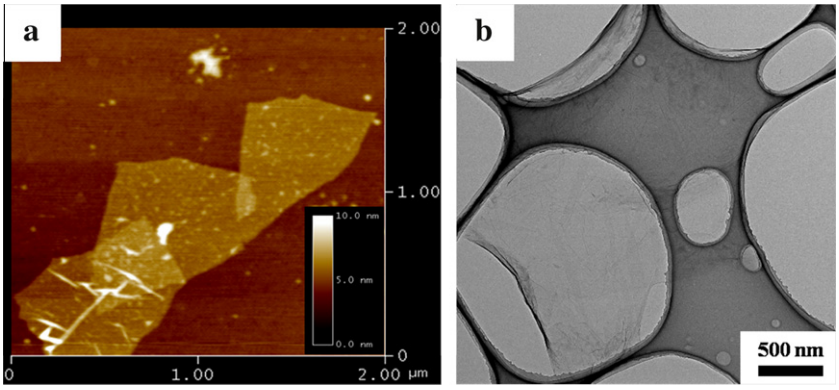

Fig. 2 – AFM data (a) and TEM image (b) of graphene oxide.

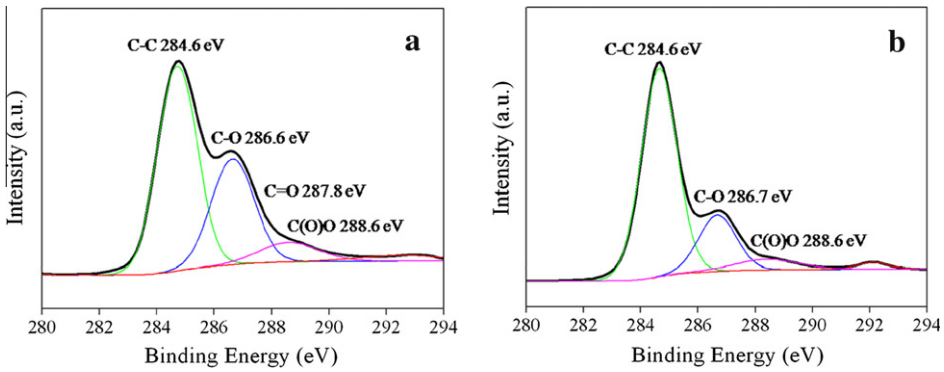

Fig. 4 – Typical C 1s XP spectra of graphene oxide (a) and alkylated graphene oxide (b).

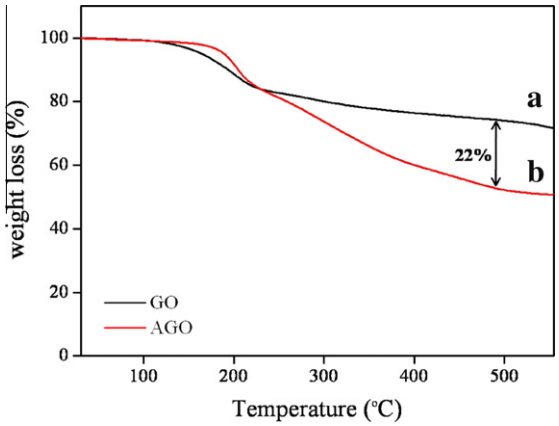

Fig. 5 – TGA data of graphene oxide (a) and alkylated graphene oxide (b).

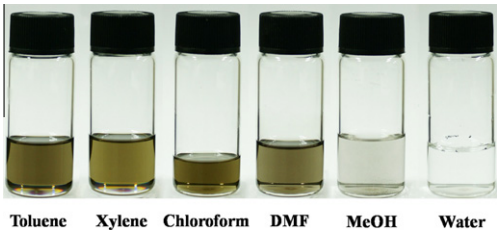

Fig. 6 – Optical image of alkylated graphene oxide dispersions in different solvents (0.01 mg AGO/10 g solution).

The thermal degradation of PP and the AGO/PP composites was examined by determining the mass loss during heating. Fig. 7(a) presents the mass loss curves of the samples at a heating rate of 10 °C/min. During thermal degradation, the samples exhibited a single step degradation behavior. The mass loss curve of homo PP showed a 10 wt% weight loss at approximately 402.08 °C. In addition, with increasing AGO content, thermal degradation temperatures (TDTs) of the AGO/PP composites increased gradually. The TDTs of a 1 wt% AGO-incorporated PP composite were increased by more than 33 °C. This sharp increase was attributed to the reduced thermal contact resistance at the interface, which is a barrier to heat transfer and reduces the overall effective thermal conductivity. One key reason for the high interfacial resistance is the weak bonding between polymer matrix and filler. Since thermal energy is transferred mainly in the form of lattice vibration (phonons), poor coupling in the vibration modes at the filler-polymer matrix interfaces will impart significant interfacial resistance. AGO containing a large number of alkyl chains exhibited good interfacial adhesion with the hydrophobic PP matrix. The good interfacial adhesion of AGO resulted in a decrease in interfacial resistance between AGO and the PP matrix. In addition, the good dispersibility of AGO in PP matrix could maximize the interfacial area between the AGO and PP matrix. Therefore, layers of PP matrix with a low thermal conductivity were being thinned by the homogeneous exfoliation of AGO, which has a two-dimensional structure and large surface area. As a result, the TDTs of the PP/AGO composites were increased considerably. In addition, the high aspect ratio of AGO led to higher thermal conductivity by inducing a much lower percolation threshold in the PP/AGO composites. This also contributed the enhanced TDTs. Fig. 7(b) shows the differences in the thermal degradation behavior between one-dimensional alkylated carbon nanotube (ACNT)-reinforced PP composites and two-dimensional AGO-reinforced composites. At a 0.5 wt% filler content, the TDTs of the ACNT-incorporated PP composites was increased by more than 16 °C compared to that of the homo PP. This enhancement was induced by the high thermal conductivity of percolated ACNT. In contrast, the TDTs of the AGO incorporated PP composite was increased by more than 24 °C compared to that of homo PP. The better performance of AGO in the TDTs was attributed to stronger interfacial adhesion by the large number of alkyl groups on AGO with a large surface area and high aspect ratio.

Fig. 8(a) shows the DSC thermograms of the 1st cooling stage of the AGO/PP composites. The re-crystallization temperatures of the composites increased gradually with increasing AGO content. This suggests that AGO acts as a nucleation agent for crystallization of the PP matrix by providing a very large surface area for adsorption of the PP chain, resulting in easier nucleation. This behavior is similar to a previous report by Layek et al. [28]. However, the nucleating ability of AGO is inferior to that of ACNT (Figure 8(b)).

Table 1 lists the thermal properties of the AGO and ACNT-reinforced PP composites. The overall thermal properties of the composites were enhanced by AGO. In particular, despite the low filler content, the sharp increase in TDTs was interesting. Fig. 9 shows the mechanical properties of the AGO

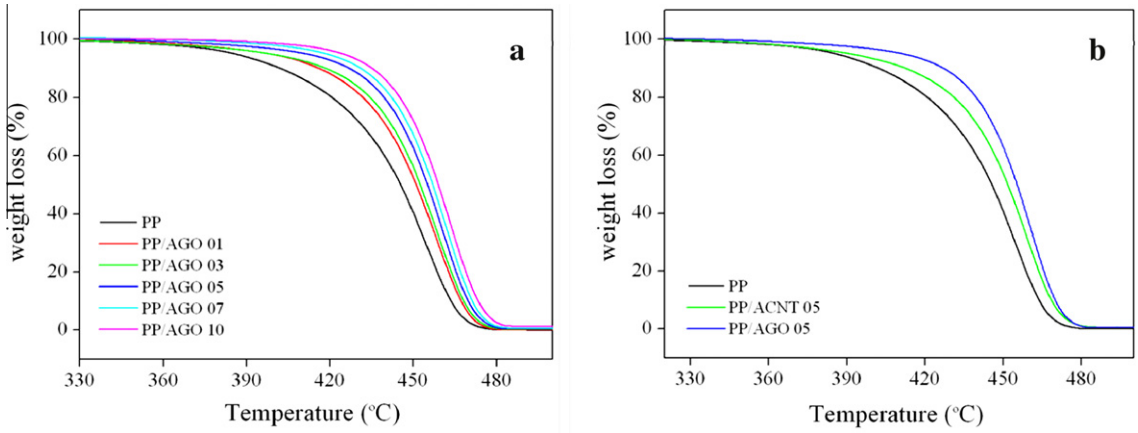

Fig. 7 – TGA data of alkylated graphene oxide/polypropylene composites (a) and different carbon fillers/polypropylene composites (b).

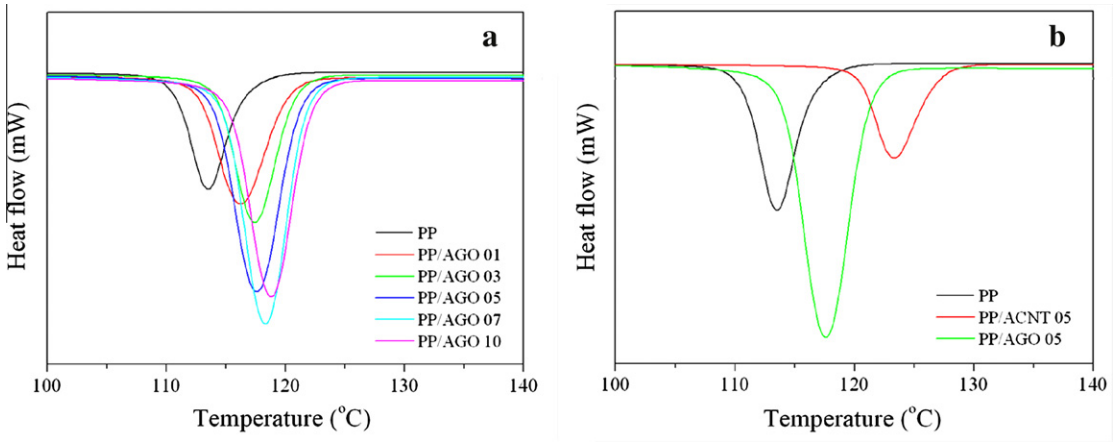

Fig. 8 – DSC data of alkylated graphene oxide/polypropylene composites (a) and different carbon fillers/polypropylene composites (b).

and ACNT-reinforced PP composites. From the standpoint of mechanical properties, AGO is only beneficial to the Young's modulus of the composites. The tensile strength and strain to maximum decreased gradually with increasing AGO content compared to those values of homo PP. However, the Young's modulus of the AGO/PP composites increased considerably. Only 0.1 wt% AGO was needed to increase the Young's modulus of the composite by more than 70%. The enhanced the Young's modulus is due to the greater stiffness contrast between AGO and the PP matrix. An interaction between the alkyl groups of AGO and the PP matrix as well as the mechanical interlocking at the wrinkled surface restrict segmental mobility of the polymer chains near the AGO surfaces. For glassy polymers, similar results were obtained from PMMA (33% improvement at only 0.01 wt%) [22] and epoxy (31% increase at 0.1 wt%) [19] reinforced with TRG. In contrast, the decrease in tensile strength and strain to maximum indicates that the molecular rearrangement and orientation with respect to the tensile axis during deformation are inhibited in the presence of AGO. The reduced segmental mobility of the PP/AGO composites resulted in those decreases in tensile strength and strain to maximum. In the case of the ACNT incorporated composite, a filler content of 0.5 wt% was needed to increase the tensile strength and Young's modulus of the ACNT-incorporated composites by 20% and 37%, respectively. These differences between AGO and ACNT in the composites were induced by their morphological differences. Two-dimensional AGO with a large surface area and high aspect ratio has a stronger interaction with the PP matrix. Although the strong interaction between AGO and

Table 1 – Thermal properties of the alkylated graphene oxide/polypropylene composites and alkylated carbon nanotube/polypropylene composites.

Sample name	T_c (°C)	T_m (°C)	T_d (°C)
PP	113.51	158.80	402.08
AGO-01/PP	116.20	160.26	415.91
AGO-03/PP	117.39	161.08	418.46
AGO-05/PP	117.55	161.49	426.98
AGO-07/PP	118.29	161.45	431.11
AGO-10/PP	118.89	161.85	435.15
ACNT-05/PP	123.41	163.13	418.46

T_d: 10 wt% loss.

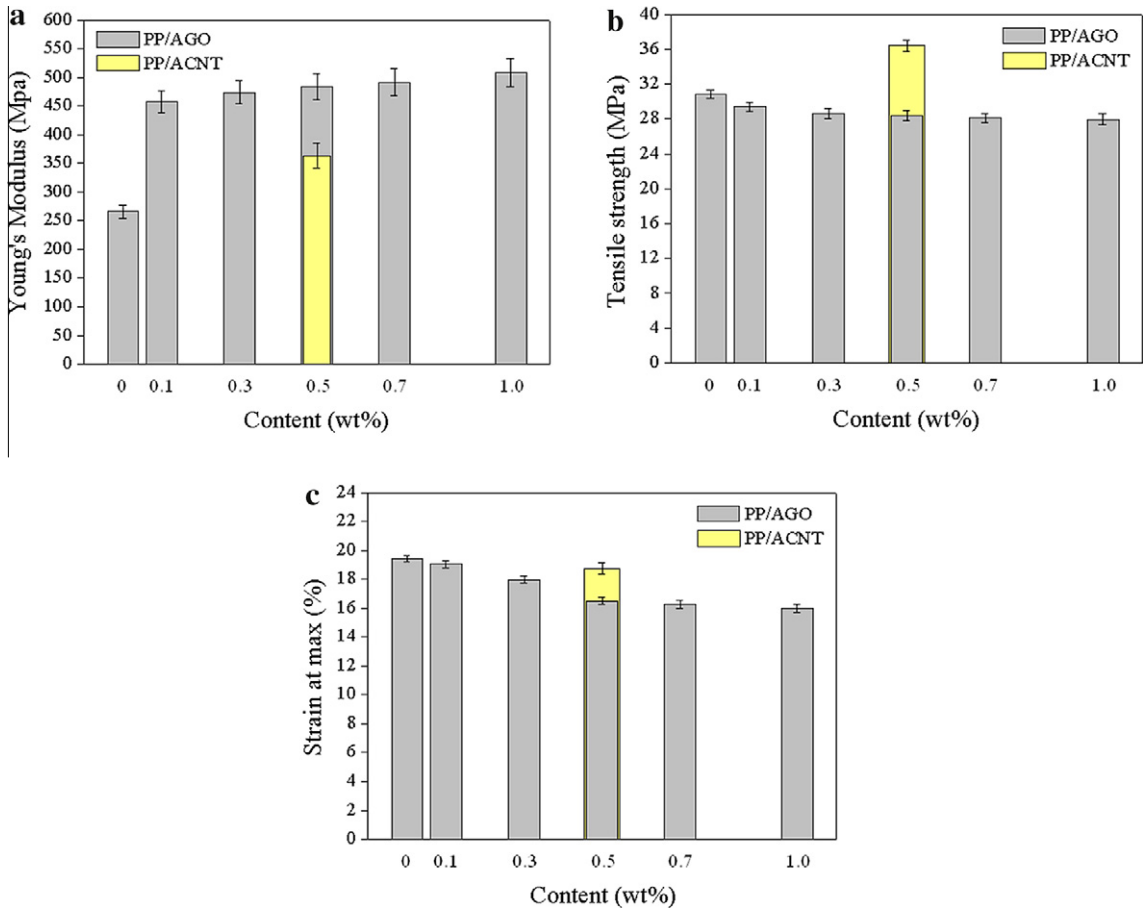

Fig. 9 – Mechanical properties of the alkylated graphene oxide/polypropylene composites and alkylated carbon nanotube/polypropylene composites.

PP matrix compared to that of ACNT resulted in significant enhancement of the Young's modulus, it brought about a decrease in tensile strength, which is in contrast to that observed with ACNT. These differences between AGO and ACNT in the composites are interesting. According to the shapes of the nano-sized fillers, the reinforcing effects on the composite were obviously different. This suggests that a dual or triple filler system might be more effective on the composites than a single filler system.

4. Summary

This study examined the reinforcing effects of AGO on a non-polar polypropylene matrix and compared these effects with those of one-dimensional CNT. The GO surface was modified with a linear alkyl chain through an S_N2 reaction between the oxygen groups of GO and the reactants to promote the homogeneous dispersion of GO in an organic solvent and increase the interfacial adhesion between GO and the non-polar polymer matrix. The AGO was dispersed homogeneously in non-polar solvents containing xylene but not in the polar solvents, such as methanol and water. The AGO/PP composites were prepared using AGO dispersions in xylene. The TDTs, re-crystallization temperatures and Young's modulus of the composites increased gradually with increasing AGO content. In particular, the TDTs of the AGO incorporated PP composite were increased by more than 33 °C at a 1 wt% AGO loading, and only 0.1 wt% AGO was needed to increase the Young's modulus of the composite by more than 70%. These reinforcing effects of AGO were different from those of one-dimensional ACNT. The two-dimensional structure of AGO with a large surface area and high aspect ratio is advantageous in that it allows overlap and provides a large interaction area between the AGO and PP matrix of the composite. Therefore, the reinforcing effects of AGO are superior to those of ACNT in terms of the TDT and Young's modulus of the composites.

Acknowledgment

This work was supported by the National Research Foundation of Korea Grant funded by the Korean Government (MEST) (NRF-2010-C1AAA001-0029018).

REFERENCES

[1] Kang M, Myung SJ, Jin HJ. Nylon 610 and carbon nanotube composite by in situ interfacial polymerization. Polymer 2006;47(11):3961–6.

[2] Mucha M, Marszałek J, Fidrych A. Crystallization of isotactic polypropylene containing carbon black as a filler. Polymer 2000;41(11):4137–42.
[3] Krupa I, Chodák I. Physical properties of thermoplastic/graphite composites. Eur Polym J 2001;37(11):2159–68.
[4] Yun YS, Kwon HI, Bak H, Lee EJ, Yoon JS, Jin HJ. Morphological effects of alkylated multiwalled carbon nanotubes on poly(L-lactic acid)-based composites. Macromol Res 2010;18(9):828–33.
[5] Lee HS, Yun CH, Kim HM, Lee CJ. Persistence length multiwalled carbon nanotubes with static bending. J Phys Chem C 2007;111(50):18882–7.
[6] Lee HS, Yun CH, Kim SK, Choi JH, Lee CJ, Jin HJ, et al. Percolation of two-dimensional multiwall carbon nanotube networks. Appl Phys Lett 2009;95(13):134103–4.
[7] Song PC, Liu CH, Fan SS. Improving the thermal conductivity of nanocomposites by increasing the length efficiency of loading carbon nanotubes. Appl Phys Lett 2006;88(15):153111–3.
[8] Dikin DA, Stankovich S, Zimney EJ, Piner RD, Dommett GHB, Evmenenko G, et al. Prepatation an characterization of graphene oxide paper. Nature 2007;448(7152):457–60.
[9] Li D, Müller MB, Gilje S, Kaner RB, Wallace GG. Processable aqueous dispersions of graphene nanosheets. Nature Nanotech 2008;3(2):101–5.
[10] Stankvich S, Dikin DA, Dommett GHB, Kohlhaas KM, Zimney EJ, Stach EA, et al. Graphene-based composite materials. Nature 2006;442(7099):282–6.
[11] Niyogi S, Bekyarova E, Itkis ME, McWilliams JL, Hamon MA, Haddon RC. Solution properties of graphite and graphene. J Am Chem Soc 2006;128(24):7720–1.
[12] Wang X, Tabakman SM, Dai H. Atomic later deposition of metal oxides on pristine and functionalized graphene. J Am Chem Soc 2008;130(26):8152–3.
[13] Subrahmanyam KS, Vivekchand SRC, Govindaraj A, Rao CNR. A study of graphenes prepared by different methods: characterization, properties and solubilization. J Mater Chem 2008;18(13):1517–23.
[14] Soldano C, Mahmood A, Dujardin E. Production, properties and potential of graphene. Carbon 2010;48(8):2127–50.
[15] Kim H, Abdala AA, Macosko CW. Graphene/polymer nanocomposites. Macromolecules 2010;43(16):6515–30.
[16] Vadukumpully S, Paul J, Mahanta N, Valiyaveettil S. Flexible conductive graphene/poly(vinyl chloride) composite thin films with high mechanical strength and thermal stability. Carbon 2011;49(1):198–205.
[17] Stankovich S, Dikin DA, Dommett GHB, Kohlhaas KM, Zimney EJ, Stach EA, et al. Graphene-based composite materials. Nature 2006;442(20):282–6.
[18] Veca LM, Meziani MJ, Wang W, Wang X, Lu F, Zhang P, et al. Carbon nanosheets for polymeric nanocomposites with high thermal conductivity. Adv Mater 2009;21(20):2088–92.
[19] Rafiee MA, Rafiee J, Wang Z, Song H, Yu Z-Z, Koratkar N. Enhanced mechanical properties of nanocomposites at low graphene content. ACS Nano 2009;3(12):3884–90.
[20] Lerf A, He H, Forster M, Klinowski J. Structure of graphene oxide revisited. J Phys Chem B 1998;102(23):4477–82.
[21] Boukhvalov DW, Katsnelson MI. Modeling of graphite oxide. J Am Chem Soc 2008;130(32):10697–701.
[22] Ramanathan T, Abdala AA, Stankovich S, Dikin DA, Herrera-Alonso M, Piner RD, et al. Functional ized graphene sheets for polymer nanocomposites. Nature Nanotech 2008;3(6):327–31.
[23] Stankovich S, Piner RD, Nguyen ST, Ruoff RS. Synthesis and exfoliation of isocuanate-treated graphene oxide nanoplastelets. Carbon 2006;44(15):3342–7.
[24] Park S, Dikin DA, Nguyen ST, Ruoff RS. Graphene oxide sheets chemically cross-linked by polyallylamine. J Phys Chem C 2009;113(36):15801–4.
[25] Park S, An J, Jung L, Piner RD, An SJ, Li X, et al. Colloidal suspensions of highly reduced graphene oxide in a wide variety of organic solvents. Nano Lett 2009;9(4):1593–7.
[26] Paredes JI, Villar-Rodil S, Martinez-Alonso A, Tascón JMD. Graphene oxide dispersions in organic solvents. Langmuir 2008;24(19):10560–4.
[27] Park S, Ruoff RS. Chemical methods for the production of graphenes. Nature Nanotech 2009;4(4):217–24.
[28] Layek RK, Samanta S, Chatterjee DP, Nandi AK. Physical and mechanical properties of poly(methyl methacrylate)–functionalized graphene/poly(vinylidine fluoride) nanocomposites: piezoelectric b polymorph formation. Polymer 2010;51(24):5846–56.